K.–D. BOUZAKIS, N. MICHAILIDIS,
K. EFSTATHIOU, S. HADJIYIANNIS, G. SKORDARIS

UDK 621.9.025.004.6

RESEARCH

Mechanical Properties, Fatigue Failure and Milling Performance of Coated Tools, Investigated Through Innovative FEM Supported Experimental Procedures

The fatigue and the wear behavior of coatings on cemented carbide substrates are investigated experimentally in milling and analytically through a Finite Elements Method (FEM) simulation of the cutting process. The hereby required coatings and substrates mechanical properties are determined by means of an innovative FEM supported evaluation procedure of nanoindentation test results. Critical coating fatigue stresses were experimentally found out through the impact test and are taken into account in the interpretation of the coated inserts cutting performance. Substrate surface mechanical treatments, such as micro-blasting and cutting edge rounding, convenient coating annealings and appropriate coating materials, are some of the investigated cases. The initiation and progress of the tool failure is depicted through Scanning Electron Microscopy (SEM) and Energy Dispersive X-ray microspectral investigations of the used cutting edges. Furthermore the FEM simulation of the contact between the tool and the workpiece enables a quantitative description of the influence of mechanical stress components on the coating failure. Coating stress-strain properties determined as mentioned through the FEM supported nanoindentation results evaluation method are considered in the impact test simulation.

Keywords: *Milling, PVD coatings cutting performance, Nanoindentation, Cutting wedge radius, Feedrate*

1. *INTRODUCTION*

The increasing manufacturing demands, being supported by the improved capabilities of modern machine tools, require the persistent evolution of superior materials for cutting tools. The milling performance of cemented carbide tools, was impressively improved by the development of advanced coating systems /1,2,3,4/. The progress of the Physical Vapor Deposition (PVD) as a thin film production technique is the reason for the further broad diffusion of such coatings /5/. Nowadays, advanced and complicated techniques are incorporated in film production systems, leading in this way to the development of an extended variety of different coating types, so that soft, hard and superhard coatings with superior properties can be produced.

2. COATINGS MECHANICAL AND FATIGUE PROPERTIES DETERMINATION BY MEANS OF NANOINDENTATIONS AND IMPACT TESTS RESPECTIVELY

The nanohardness measurement is a precise indentation method to monitor continuously the course of the penetration depth versus the applied indentation force. This measurement consists of two steps, the so-called loading stage and the relaxation one (see figure 1). During the loading stage, a load forces a diamond indenter to penetrate into the specimen. This load is gradually applied and at the same time both the actual indentation force and depth are registered, as presented in the upper right part of the figure. When the load is removed (relaxation stage), due to the resulting material plastic deformation, there is a remaining depth hP. By means of a Finite Elements Method (FEM) continuous simulation of the indentation procedure previously described, coating stress strain curves can be determined (algorithm "SSCUBONI" (Stress Strain CUrves Based On NanoIndentations) [6]). The applied FEM model of the semi-infinite layered half space was considered to be axisymmetric, as illustrated in the bottom part of the same figure. The stress strain curve determined, has in generally three distinct areas: the elasticity, the small and the large scale plasticity areas, corresponding to concrete regions of the indentation depth versus load curve, as shown in the upper right figure part.

The curve during the loading stage is digitalized in a number of Fi-hi pairs, as the corresponding table in the lower figure part demonstrates. These values are the input data to the developed "SSCUBONI" algorithm. The corresponding stress strain distributions to the numbered from I up to IV Fi-hi pairs, determined through the SSCUBONI algorithm, are illustrated in figure 2.

K.–D. Bouzakis, N. Michailidis, K. Efstathiou, S. Hadjiyiannis, G. Skordaris
Laboratory for Machine Tools and Manufacturing Engineering, Mechanical Engineering Department, Aristoteles University of Thessaloniki, 54006 Thessaloniki, Greece

The paper was published at Seventh Yugoslav Tribology Conference YUTRIB 2001

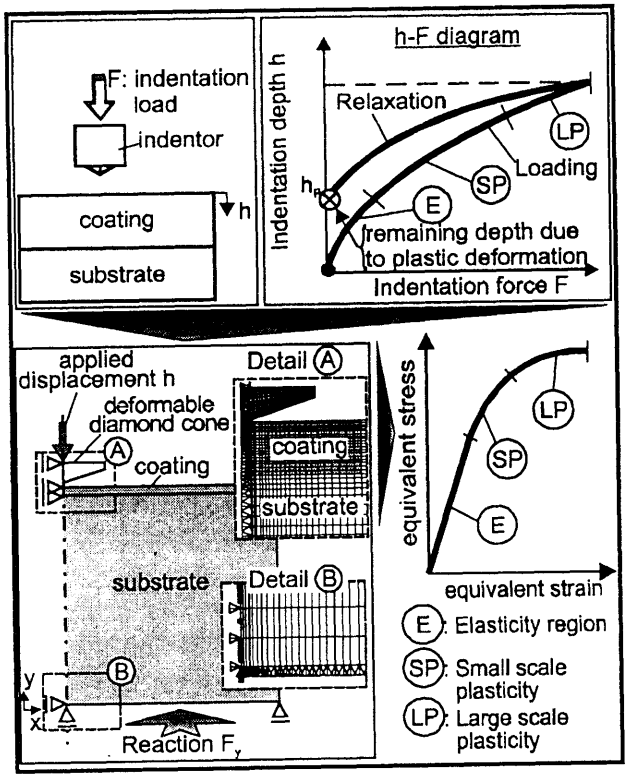

Figure 1: FEM continuous simulation of the nanohardness measurement to extract coating stress strain curves

The von Mises equivalent stress distributions, determined at the penetration depths h_I to h_V and h_{VI}, are presented in the left figure part. At the same penetration stages, the occurring corresponding von Mises equivalent strain distributions in the coating are shown in the middle figure part. Owing to these stress strain distributions, by means of the introduced continuous FEM based nanoindentation simulation extracted, the coating stress strain S_{max} - ε_{max} curve is stepwise calculated as demonstrated in the right figure part.

Up to a penetration depth of approximately 40 nm, the coating is deformed purely elastic. The present nanoindentation procedure, terminates at a maximum penetration depth of 222 nm. In the corresponding stress-strain distribution graphs, the shadowed areas indicate that the coating material deformation has entered into the regions of the overall stress strain curve, shown in the lowest diagram in the right figure part [6].

The "SSCUBONI" accuracy can be among others judged, through the deviation of the calculated remaining imprint depth, due to the coating plastic deformation, from the measured one, which is less than approximately 2%. Through the assumption that the coating behaves purely elastic, coating failure mechanisms, observed for example during the impact test, could not be explained. On the other hand, as it will be described in the following section, the consideration of the whole coating elastic plastic stress strain behavior enables the interpretation of such coating fracture phenomena.

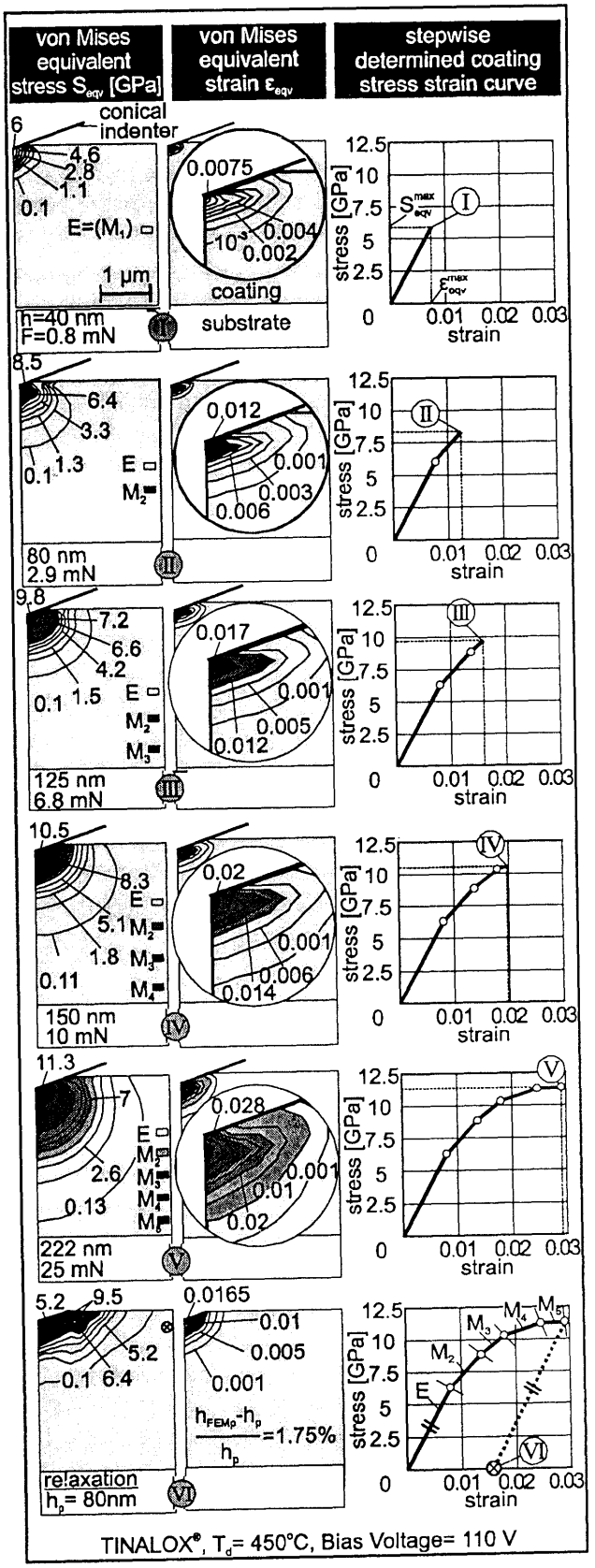

Figure 2: Stress and strain distributions during the nanoindentation test, calculated through the FEM supported continuous simulation of the nanoindentation test ("SSCUBONI" algorithm) and the herewith-determined stress strain curves.

An improved construction of the impact tester is shown in figure 3. During the impact test a carbide ball penetrates under a desired maximum loading level into the coating, periodically. Due to the plastic deformation that develops during the loading stage, the contact area does not fully recover to its initial plane shape, forming herewith a permanent concave imprint. The coating failure mode can be either cohesive or adhesive. For well adherent coatings, the major fatigue danger is the cohesive one, i.e. intrinsic coherence release and microchipping. For each specific set of experiments, there is a critical impact load associated to 106 successive impacts, which the coating withstands without failure. In the bottom figure part according to the impact tester working principle, its FEM simulation is illustrated /8,9/. With the aid of this FEM model, the coating stresses, associated to the critical contact load, ensuring the coating continuous endurance (fatigue strength), can be determined /8,9/.

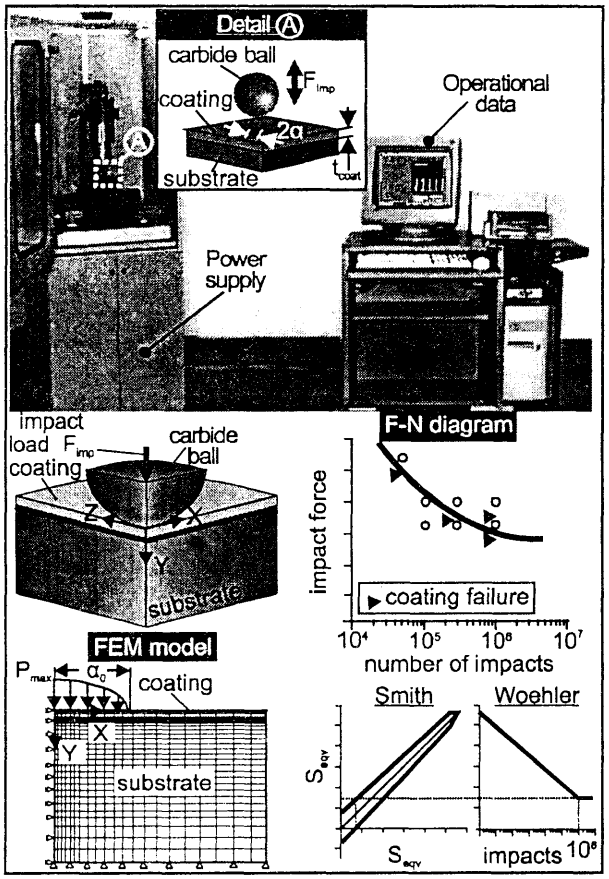

Figure 3: The Impact Test, its FEM simulation and typical Smith and Woehler diagrams, obtained by its application.

3. Parameters affecting the coated tool cutting performance and milling process simulation

Figure 4 indicates potential magnitudes influencing the cutting performance of coated tools. The effects of some of these parameters, i.e. the cutting wedge radius, the coating material properties, the coating annealing etc, on the wear behavior are described in /10,11,12,20,21/.

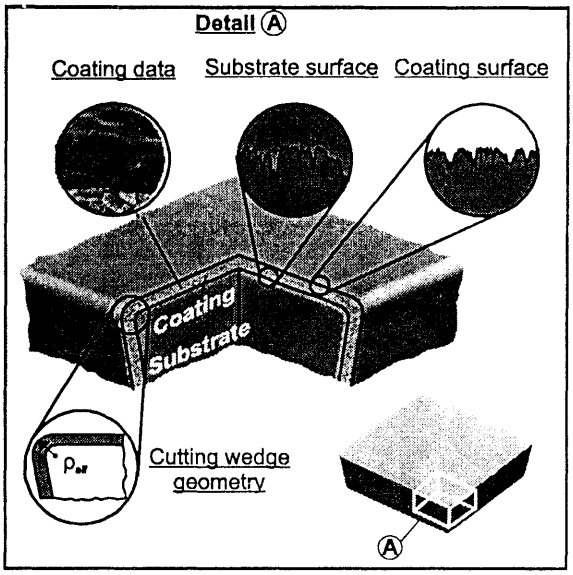

Figure 4: Parameters affecting the coated tool cutting performance.

Figure 5 illustrates the used tool-workpiece system in milling. The cutting experiments were performed using a 3-axis CNC machine center. Appropriate tool holders, according to the tool geometry were applied. A prescribed number of successive cuts was set before every examination of the cutting insert wear status. The tool wear condition was monitored by means of optical and SEM investigations. During the cutting process, besides the tool wear observation, further significant process parameters, such as the cutting force components were monitored. The used workpiece material was 42CrMo4 hardened steel, whose mechanical properties and chemical composition are inserted at the bottom part of the same figure.

The FEM modeling strategy of the coated cutting wedge and of its loads during the material removal process is illustrated in figure 6. According to the tool holder the tool-workpiece system is simulated considering the corresponding cutting kinematics, shown at the upper right part of this figure. Each of the shown tool holder cases is generally described by a plain strain model of the coated cutting wedge, illustrated at the bottom part

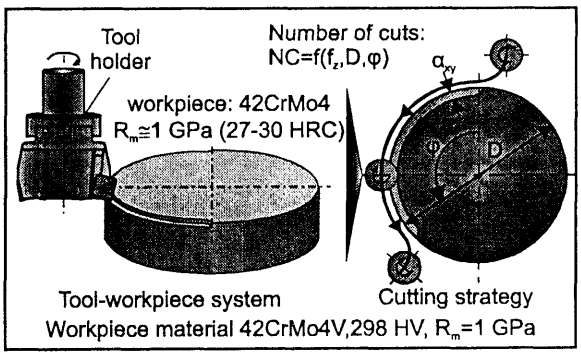

Figure 5: Milling process kinematics and workpiece material properties.

of the same figure. The acting cutting loads are applied in a form of superficial normal and tangential pressure distributions, determined considering the entire cutting kinematics, the measured cutting forces and the chip compression ratio. To create a reproducible model, capable of prescribing stress distributions, independent of geometric and dynamic restrictions the simulation was parametrically built. Thus, the coating thickness, the chip dimensions, the cutting loads and the model dimensions are variable and changeable parameters, using a design language that the employed FEM package supports /13/.

4. The effect of the substrate cutting wedge radius on its milling performance

The cemented carbides, considering their structure and composition may express anisotropic and inhomogeneous behaviour /14,15/. On that account their strength in tension and compression is different and the von Mises failure criteria are not valid. Considering this fact, the tool designers pay attention on the tool cutting geometry in order to avoid concentrations of high principal stresses, especially of tensile ones, capable to provoke brittle cutting edge microbreakages that may deteriorate the tool performance. At a first stage of experiments with hardmetal substrates, coated inserts were used having a relatively sharp cutting edge rounding, filleted with radius of 4 μm /14/. For this case, the experimental results illustrated a very early failure of the tip of the cutting edge, due to reasons explained in the further paragraphs. To solve this problem a different, larger radius was selected and the experimental cutting edge stability was improved.

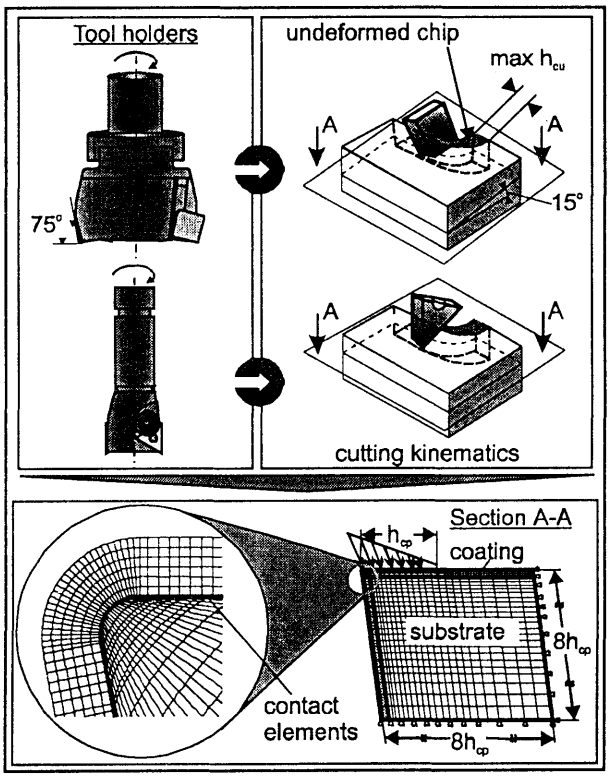

Figure 6: FEM simulation model of the milling process considering the tool holder.

The left part of figure 7 illustrates the stress behaviour of a sharp cutting edge, which has a filleted tip by a small radius of 4 μm. The stress distributions refer to an uncoated cutting edge in order to understand that the instability of the base material is responsible for early tip microbreakages. A high concentration of tensile stresses at the flank and of compressive ones on the rake face, create a three dimensional bending field capable of breaking the cutting wedge tip at a very early number of successive cuts. These high principal tensile and compressive stress concentrations generate the two maxima of the von Mises stress, as it can be observed in the corresponding contours. This stress behaviour leads to failures of the tip of the cutting edge, similar to the corresponding one presented in the SEM micrograph of the same figure.

When a greater cutting edge rounding is applied, the stress distribution is different and illustrates only a local maximum near the beginning of the fillet at the flank (see the right part of figure 7). This stress concentration is mainly consisting of compressive principal stresses, which are not so critical for hardmetals. The aforementioned stress results verify adequately the well known experience based on the technique of forming

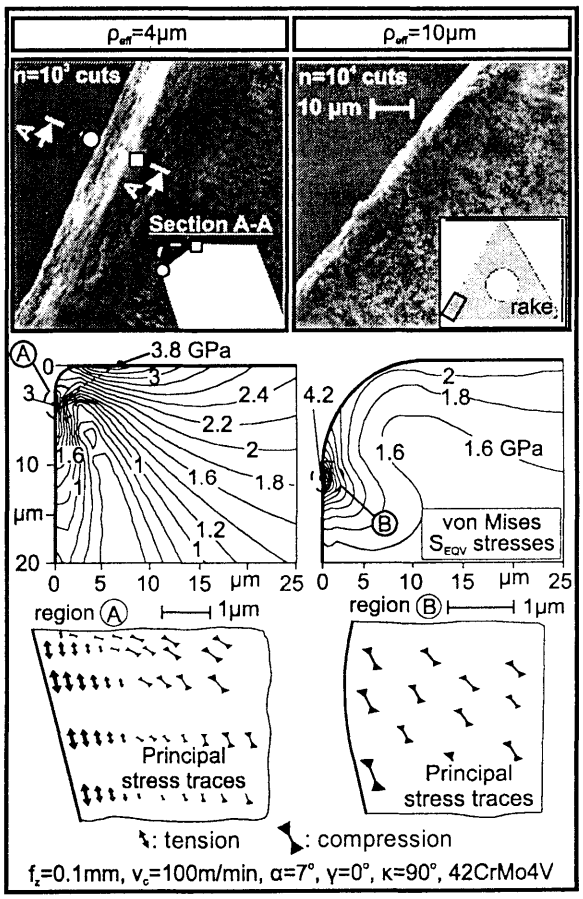

Figure 7: The effect of the cemented carbide insert ρeff modification on the stress development at the cutting wedge.

round fillets in cutting edges, to reach a stable cutting performance. This problem is not so critical in HSS substrates, taking into account their isotropy and homogeneity that ensures the application of the von Mises failure criteria, but it may occur in cases of high clearance and rake angles. As it can be observed in the SEM micrograph of the same figure for the insert of the geometry corresponding to the one illustrated in the previous geometry, but with an adequate fillet of 10 μm, the cutting edge can withstand a significant number of successive cuts, without any damage. The cutting conditions in this case were identical to the ones for the insert with the sharper cutting edge.

4.1. Premature coating failure due to small cutting wedge radius

Sharp cutting edges, are subjected to the risk of a premature coating failure at the tool tip, where stress concentrations might lead to a cohesive failure on the transient filleted flank cutting wedge region /16,17/. The FEM model described in figure 3 is applied to determine the occurring stress state. The calculated von Mises equivalent stress distribution, in the case of 5 μm effective cutting radius, is inserted in the upper part of figure 8 and corresponds to a milling operation with an unaffected cutting wedge (cutting stage 1). In this case the maximum developed stress amounts 5 GPa. Inserting this stress into the TINALOX® Woehler diagram in the upper left part of the figure, it can be found out that the tool might cut approximately over 10^4 times, until a first premature coating fatigue failure occurs. In the conducted milling experiments this expected premature coating failure occurred after approximately 5000 cuts, at the inserted in the figure SEM micrograph of the cutting wedge indicates. To examine the stress distribution in the cutting wedge region after various number of successive cuts and at different stages of cutting wedge wear, the FEM model was properly modified. In this way the occurred tool tip geometry alteration, due to the coating failure and the consequent wear propagation is considered. The stress development in the cutting wedge region at different wear stages and the corresponding SEM micrographs of the real cutting wedge, are inserted in the figure. After the first coating failure, the maximum developed equivalent stress decreases and appears on the rake face (wear stage 2). On the other hand, in the failed coating regions, high cutting heat amounts penetrate into the substrate material, implying additional thermal loads. These two contradictory facts lead to a gradual tool wear propagation on the rake face as well as on the flank. In this way after 10^4 and $4x10^4$ successive cuts the cutting wedge stress state is described as illustrated in the stages 3 and 4 respectively. The corresponding flank wear development versus the accumulated number of cuts is presented in the lower left diagram of the same figure. These results show that after a coating failure the flank wear starts increasing and the tool life is restricted. An effective way to protect the coating

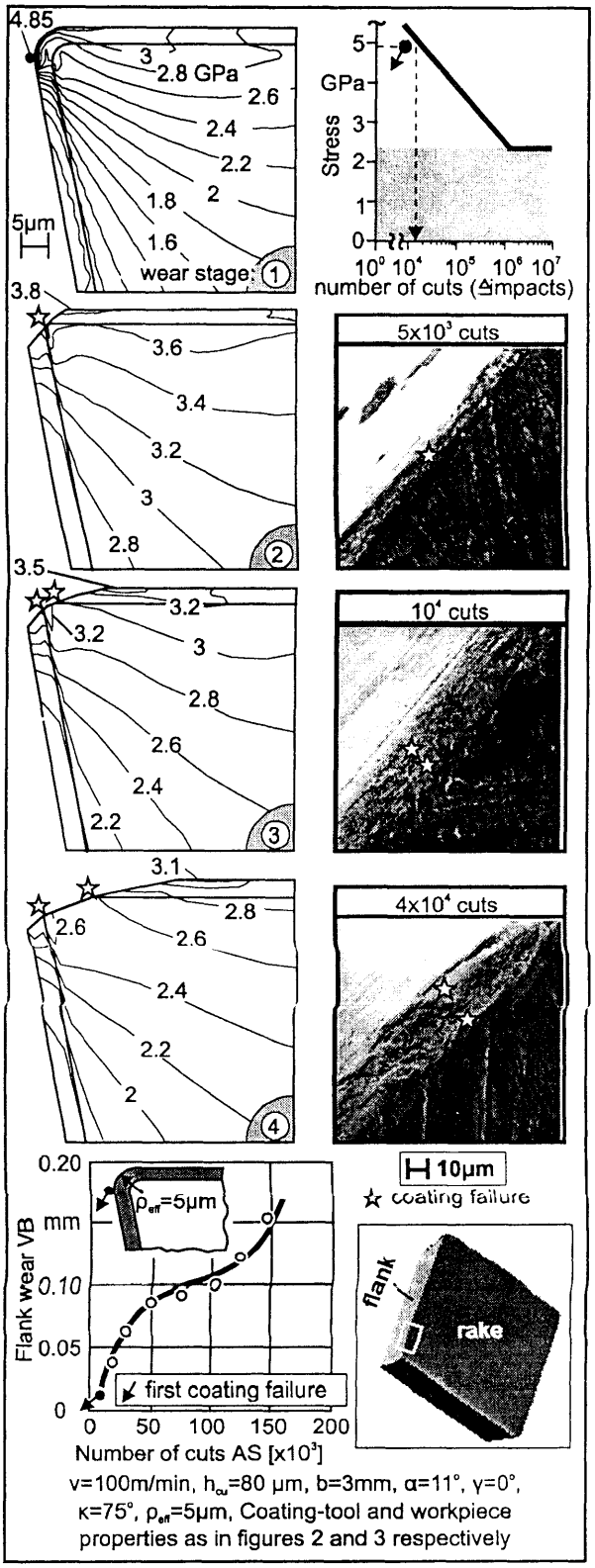

Figure 8: Premature coating fatigue failure and flank wear propagation, in milling with small cutting wedge radius

from a premature failure and the cutting insert from a consequent rapid wear propagation, is the optimization of the cutting wedge effective radius, as it will be presented in the next paragraph.

A key action to avoid the rapid wear propagation owing to a premature coating failure is to optimize the tool cutting wedge radius as well as to improve the coated tool adhesion. The effective radius of the cutting wedge consists of the cemented carbide insert radius plus the coating thickness, since the coating follows the curvature of the substrate during the deposition process. The SEM micrograph in the upper right part of figure 9 illustrates the cutting wedge after $8x10^4$ successive cuts.

The photograph is taken from an oblique viewing pointand corresponds to the initiation of coating failure at the filleted tool tip close to the flank. The failed zone of the tool flank is limited by the dashed lines and lies at the beginning of the fillet, between the rake and the flank. It is remarkable that the cutting edge, except this local coating failure, keeps its intrinsic geometry, whereas no further breakages appear. An EDX analysis verifies the coating resistance on the rake as well as the failed zone (regions A and B accordingly). The stress development presented in the middle part of this figure

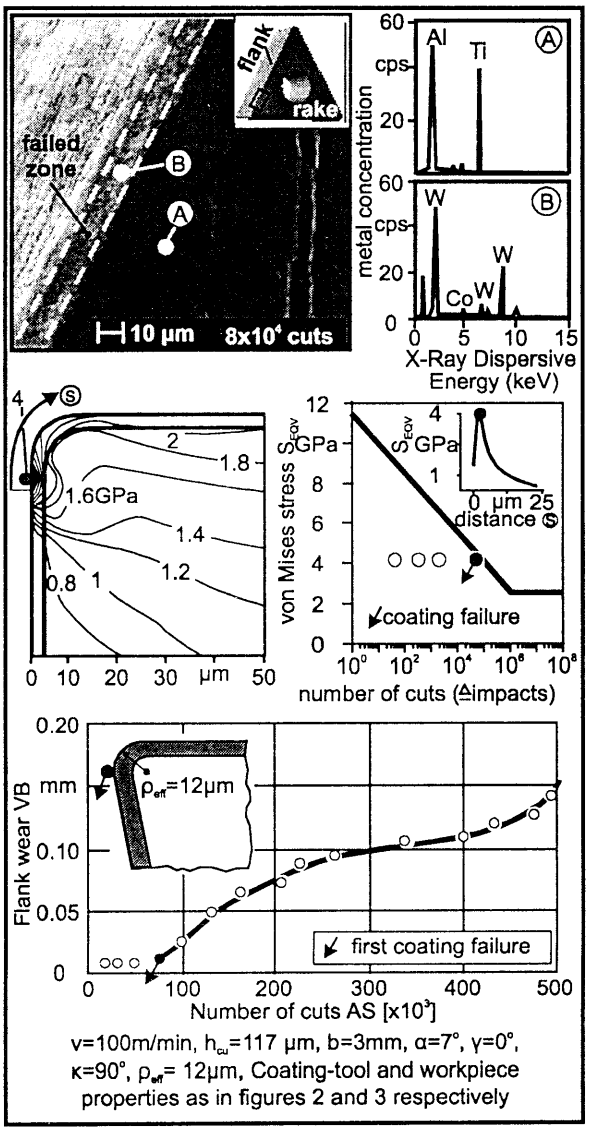

Figure 9: Coating fatigue failure and flank wear development in milling with optimized cutting wedge effective radius.

computationally sustain the observed coating failure. The region of failed coating is characterized by a local concentration of von Mises equivalent stresses. By inserting this maximum stress value in the corresponding TINALOX® Woehler diagram, it is clear that the coating resources are exhausted after approximately $8x10^4$ successive cuts. The stress distribution along the rake face is also illustrated, with the maximum stress appearing as already mentioned at the filleted tool tip close to the flank. After the first coating failure occurred in the location of the maximum stress, a flank wear propagation mechanism of the cutting wedge is initiated, as the diagram in the lower left part of the figure demonstrates.

4.2 Optimization of cutting wedge radius

The upper diagram of figure 10 shows the accumulated number of successive cuts up to the first coating failure in milling with different tool wedge radii. A decreasing of the insert cutting wedge leads to an improvement of the coating cutting time without failure. To analytically explain this experimental result, FEM supported calculations of the occurring in the coating von Mises stresses were conducted with various effective cutting wedge radii. The lower left diagram depicts the maximum calculated von Mises stress S_{eqv}^{max} versus the effective cutting wedge radius ρ_{eff}. There is a decrease of the maximum developed von Mises stress occurring through the enlargement of the wedge radius from 5 up to 12 µm. Inserting these stresses in the corresponding TINALOX® Woehler diagram, the improvement of the coating service time over the increasing of the cutting wedge radius, until a first coating failure occurs, can be found out. According to the Woehler diagram, the maximum calculated stresses correspond to numbers of cuts until the first coating failure appears, which are approximately the same with the actual ones derived from the milling experiments. The presented results also indicate that a further increasing of the effective cutting

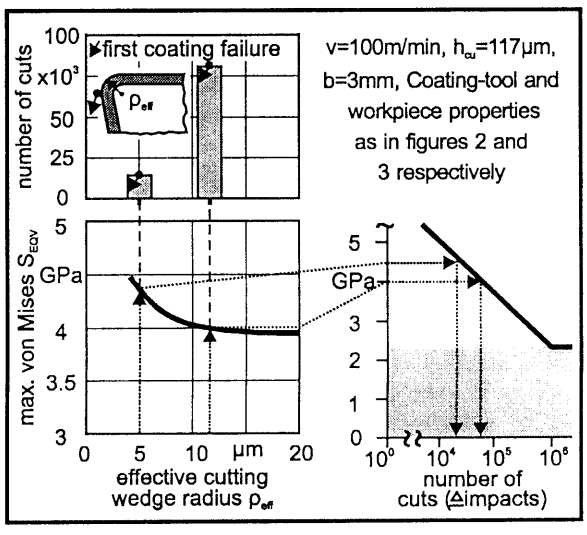

Figure 10: The effect of the cutting wedge effective radius on the maximum developed von Mises stresses and on the first coating fatigue failure.

radius over approximately 15 μm has no influence on the developed in the coating stresses and herewith its contribution on the avoidance of a coating fatigue failure is negligible.

5. Substrate surface treatments to improve the coated inserts cutting performance

To find out the influence of coated substrate surface integrity on their cutting performance, milling experiments were carried out. The cutting experiments were performed using a 3-axis numerically controlled milling center. A prescribed number of successive cuts was set before every inspection of the cutting insert wear status. The tool wear condition was monitored by means of optical and SEM investigations as well as EDX analyses for six variations of substrate surface treatments. The cutting wedge wear status for the substrate surface treatments cases such as the as deposited, micro blasted at high pressure and polished

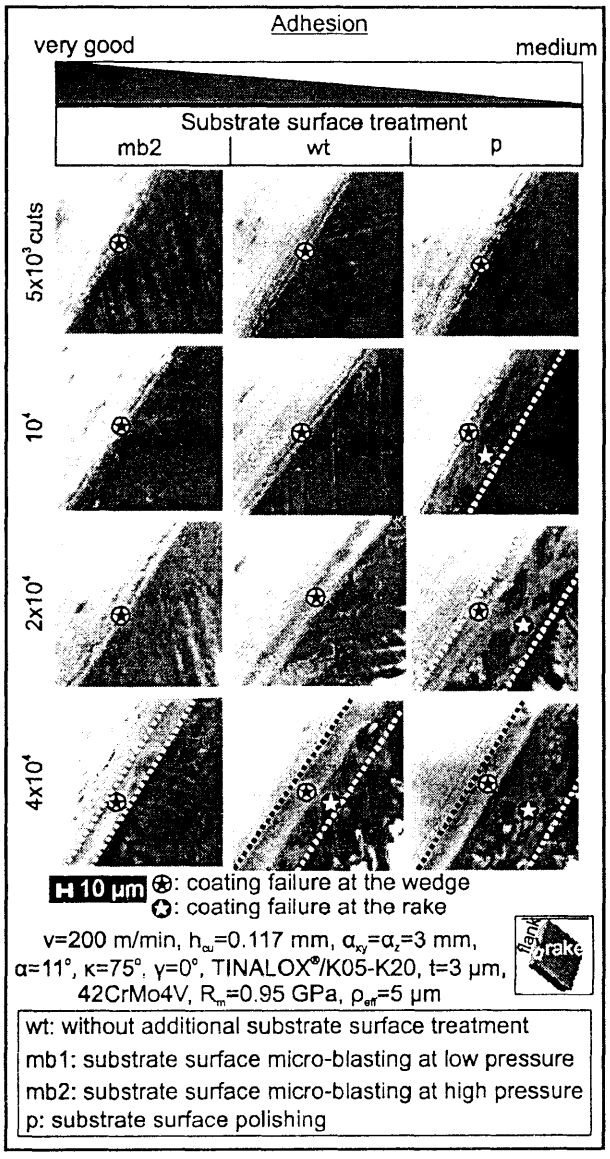

Figure 11: SEM micrographs of the examined TINALOX® coated inserts in milling, for various substrate surface treatments.

/18,19,22/, at various cutting stages is demonstrated in figure 11. As it can be observed in the SEM micrographs, the coated tool with the polished substrate has the worst wear behavior and in this case the coating is removed very soon from the tool rake in comparison to all other substrate surface treatments. Due to this fact considering the VDI and impact test results /18,19,22/ it can be stated that this wear behavior occurs through the adhesion diminishing, owing to the substrate surface polishing process. The coated insert with the untreated substrate shows a slightly improved milling performance in comparison to the polished one, while the insert treated through micro-blasting at high pressure has the overall best cutting performance mainly due to its better coating-substrate adhesion strength as already explained.

The flank wear versus the accumulated number of cuts for the examined substrate surface treatments is presented in figure 12. The flank wear was monitored by means of an optical microscope. The less intense wear increasing in the conducted milling investigations occurs in the case of the micro-blasted at high pressure substrate surface, where almost 10^5 cuts were reached up to a flank wear of 0.15 mm. On the other hand the worst cutting behavior appears in milling with polished inserts, approximately $4.5x10^4$ cuts for the same maximum flank wear value. The other substrate surface treatments lead to wear developments between the mentioned extreme cases, as shown in the figure. The inserts without an additional surface treatment, as well as the treated through micro-blasting at a low pressure (mb1) have a sufficient coating adhesion. However, due to the existing relatively to the other treatments high

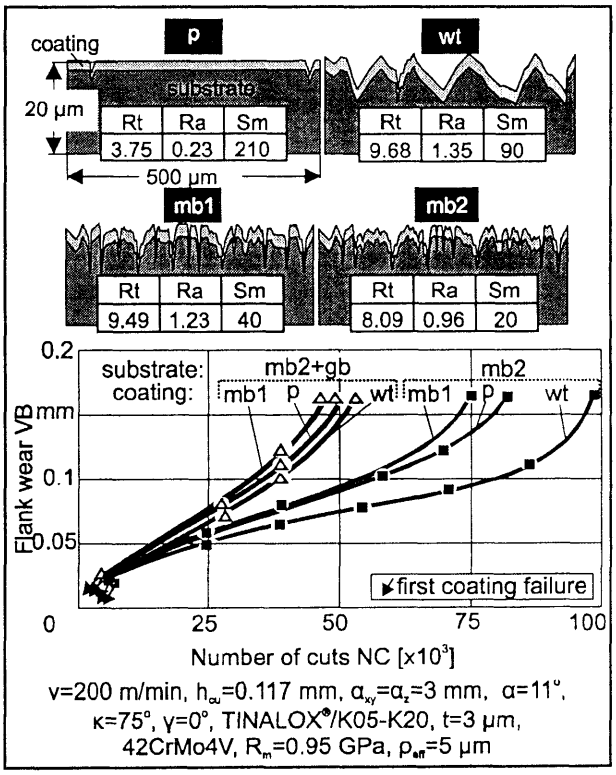

Figure 12: Coated tool flank wear development in milling, for various substrate surface treatments.

roughness picks, the coating during cutting is earlier locally failed and the tool flank and rake are not any more protected.

6 Optimization of the feedrate to improve the premature coating failure

A premature coating failure can also be avoided through optimizing the applied feedrate for a given tool geometry. In order to navigate the influence of this parameter, milling experiments at various feedrates were conducted using cutting inserts with an effective radius of 5 μm. In figure 13 the inserted SEM micrographs correspond to successive cutting wedge wear stages at various feedrates. Throughout the range of accumulated successive cuts from $5x10^3$ up to $4x10^4$, the federate leading to a maximum undeformed chip

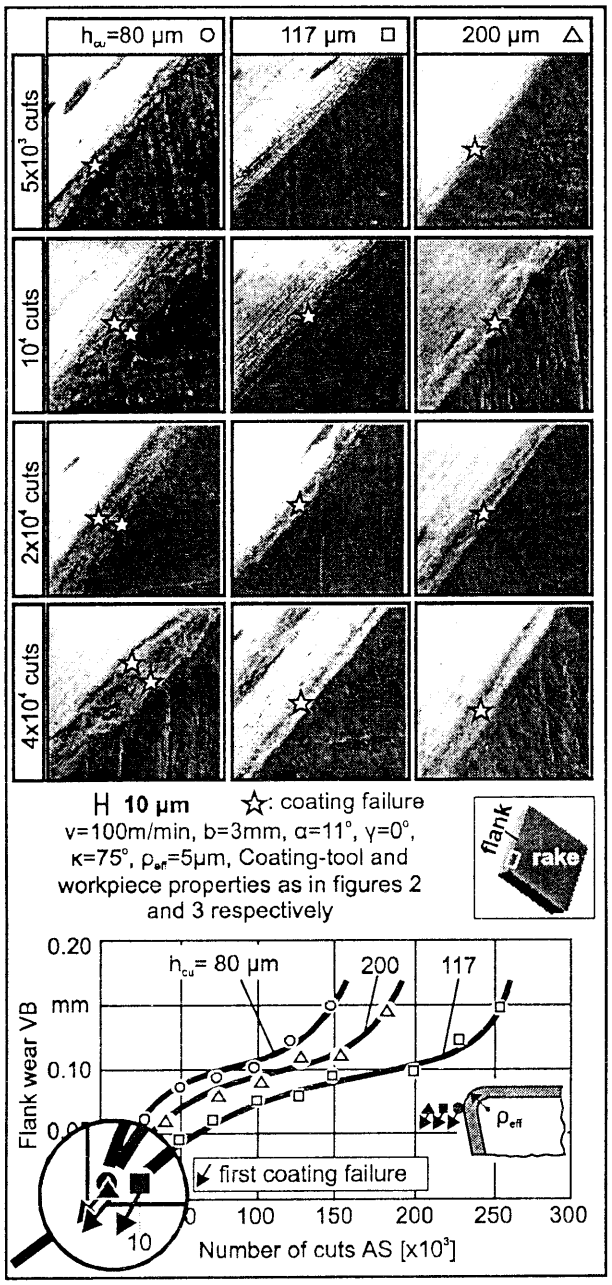

Figure 13: Coating fatigue failure and flank wear development at various feedrates.

thickness of h_{cu}=117 μm seems to have the superior behavior. Instead, in the case of h_{cu}=80 μm the worst flank wear behavior was obtained as shown in the corresponding SEM micrographs of the cutting edge after various number of cuts and in the flank wear diagram in the lower figure part. The first coating failure for both h_{cu}=80μm and 200 μm feedrate cases occurs after approximately $5x10^3$ cuts, while in the case of h_{cu}=117 μm after 10^4 cuts, according to these experimental results. Moreover the further wear propagation in the case of h_{cu}=117 μm seems to be slower in comparison to the two other feedrate cases.

To analytically sustain the experimental previous results concerning the effect of the applied feedrate on the tool performance, appropriate FEM supported stress distribution calculations were performed. In the upper part of figure 14 the developed von Mises equivalent stresses at the cutting wedge in the feedrate cases I, II and III with undeformed chip thickness 80, 117 and 200 μm respectively are inserted. The maximum developed stress in case I, leads to a tool tip overstressing and to a consequent premature failure. Feedrate cases II and III correspond to less intense cutting wedge loadings. In the left diagram of the middle part of the same figure the maximum developed von Mises equivalent stress versus the maximum applied undeformed chip thickness h_{cu} is shown. The stress in the case of h_{cu}=117 μm, gets a minimum value, which is in good agreement with the actual tool wear status presented in figure 13. The correspondence between the maximum developed

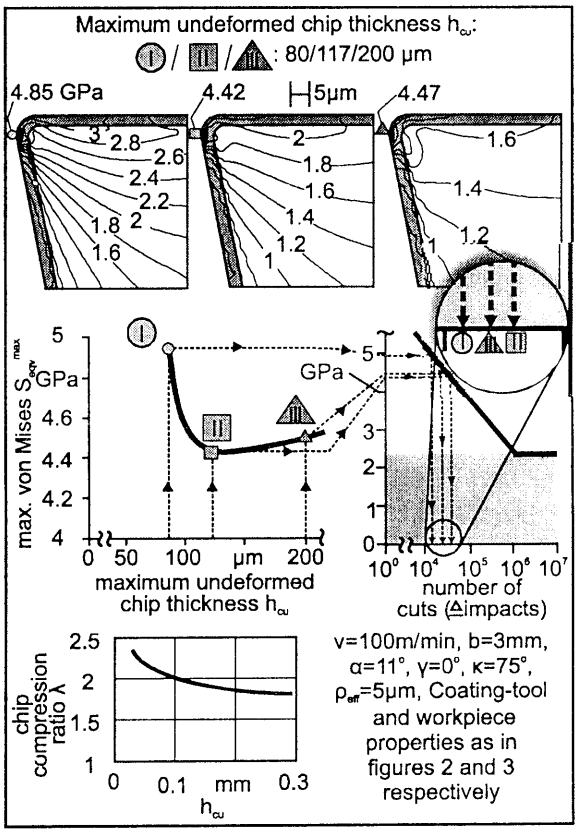

Figure 14: The effect of the applied feedrate on the maximum developed von Mises stresses and on the coating fatigue failure.

stresses and the consequent expected coating failure is performed by means of the TINALOX® Woehler diagram, depicted in the upper right diagram. In the focused area the expected number of cuts up to the first coating failure are clearly shown. From this point of view, it is clear that in the case of a feedrate corresponding to an undeformed chip thickness h_{cu}=117 μm, the expected number of cuts up to the first coating fatigue failure is higher than in the other cases with lower or higher feedrates. In the conducted FEM calculation, the parameters modification such as cutting force components and the chip compression ratio at the various feedrates were considered. The chip compression ratio alteration versus the h_{cu} is illustrated at the bottom left diagram of the figure, having a decreasing tendency with the increasing of the undeformed chip thickness.

7. Appropriate coating material selection to improve the cutting performance

To examine the influence of the coating material on the tool cutting performance, milling experiments were conducted with HSS coated inserts. Figure 15 illustrates the stress distribution within the cutting edge, during milling under the same cutting conditions. These contours refer to three examined coating cases CrN, TINALOX® and SUPERTIN®. In this position the chip exhibits its higher dimensions, with respect to the cutting kinematics. The less stiff coatings CrN and TINALOX® illustrate the maximum von Mises stresses on the rake face and near the tip of the cutting edge. On the other hand the much stiffer SUPERTIN® develops the maximum von Mises stress at a distance from the tip of the cutting edge, still on the rake face. Considering the elasticity modulus of the SUPERTIN® coating, the increasedstresses in comparison to the other investigated coatings are explained, since for the same level of the substrate and coating deformation the stresses are magnified by the increased elasticity modulus. With the aid of the presented FEM supported

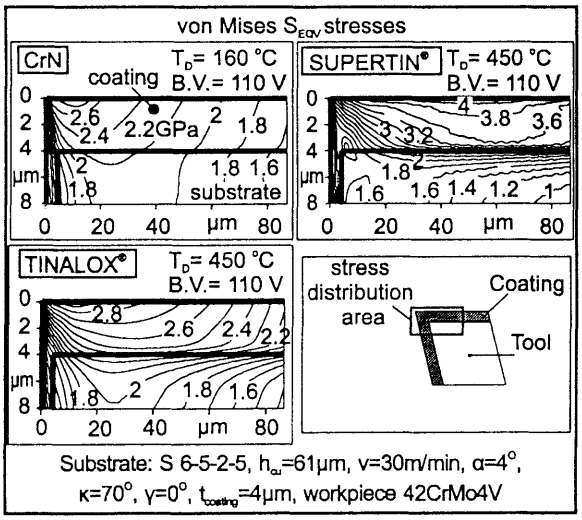

Figure 15: Stress distributions in the investigated coatings on HSS inserts under the same cutting conditions.

procedure, the maximum stresses can be predicted and compared to permitted ones, regarding the coating continuous endurance.

The experimental behaviour of the examined coatings on HSS substrate fits to the previously presented computational results. The film damages shown in the SEM photograph inserted in figure 16 for SUPERTIN® coating agree with the stress distributions presented in figure 15, where the maximum von Mises equivalent stress, significant criterion for coating fatigue failure, lies at a distance from the tip of the cutting edge of approximately 50 μm. The same region in the SEM photo illustrates failures of the coating, since the EDX microspectral analyses there (region A) indicate substrate material, i.e. high speed steel components. The superficial composition of SUPERTIN® coating without any damage is illustrated in the EDX analysis of region B of the same figure. The same figure illustrates analogous experimental results for the less stiff coating TINALOX®. The SEM photograph inserted in the upper part of the figure illustrates an early stage of the coating cohesive fatigue failure. The initiation of the coating failure is observed near the tip of the cutting edge, where a concentration of the von Mises stresses appears (see figure 15). The failure is depicted by the EDX microspectral analyses which indicate substrate components near the tip of the cutting edge. Moreover the SEM picture after 1.4x105 cuts illustrates the progress of the coating failure.

The flank wear (VB) behaviour of the investigated coatings is demonstrated in the left part of figure 17. The wear behaviour of CrN coating, having the poorest fatigue resistance is directly comparable to the HSS substrate. In the examined case, a cohesive failure was observed at a very early stage, after which the flank wear increases rapidly. This behaviour is not acceptable for coated tools and therefore soft coatings exhibiting

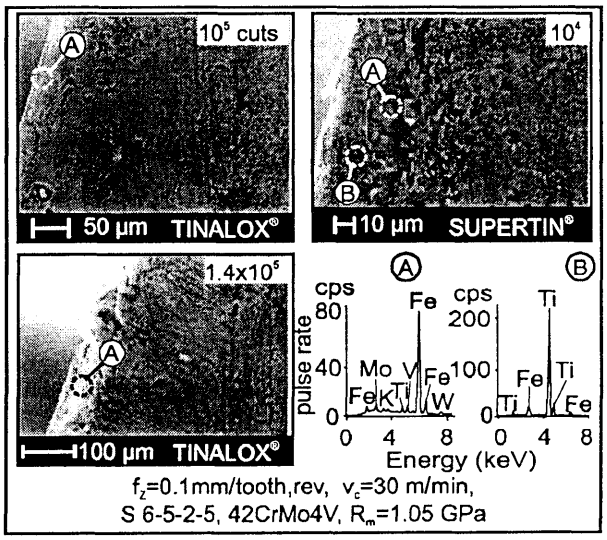

Figure 16: Failed zones on the rake face of SUPERTIN® coated HSS inserts derived by SEM and analyses as well as corresponding data for the initiation and progress of TINALOX® coating.

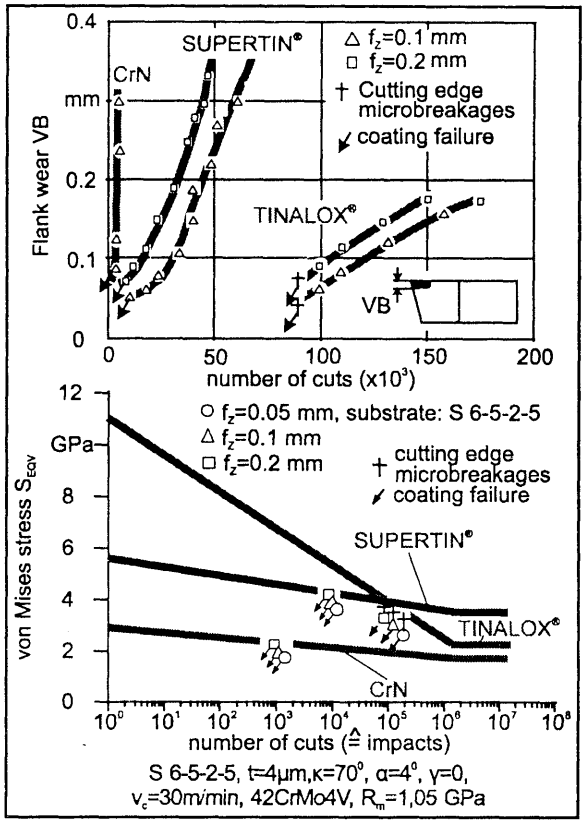

Figure 17: Flank wear versus the number of successive cuts in milling with various coated HSS inserts as well as their fatigue behavior.

poor heat and fatigue resistance, such as CrN are not recommended for cutting processes. The SUPERTIN® coating failures were observed in all investigated cases at about 10^4 successive cuts. However the coating fracture was gradual and the exposure of the substrate material lasted many successive cuts after the failure initiation. The tool managed to withstand the applied cutting loads for more than $5x10^4$ cuts with a flank wear less than 0.4 mm. In the case of TINALOX® coating, a cohesive failure was started to be visible after approximately 10^5 successive cuts. This failure was a consequence of cutting edge microbreakages, due to fatigue phenomena of the HSS substrate.

The increased hardness and wear resistance of this coating even after its failure initiation, permitted a remarkable wear resistance for the entire cutting edge. The cutting experiments with TINALOX® coated specimens were terminated in a very later stage, when the flank wear reached approximately the value 0.1 mm.

8. Cutting performance optimization through annealing

The milling experiments were conducted with as deposited and variously annealed coated inserts at a cutting speed of 100 m/min. The cutting wedge wear status was monitored by means of SEM observations and Energy Dispersive X-Ray (EDX) analyses. In figure 18 SEM micrographs of the examined cutting wedges at

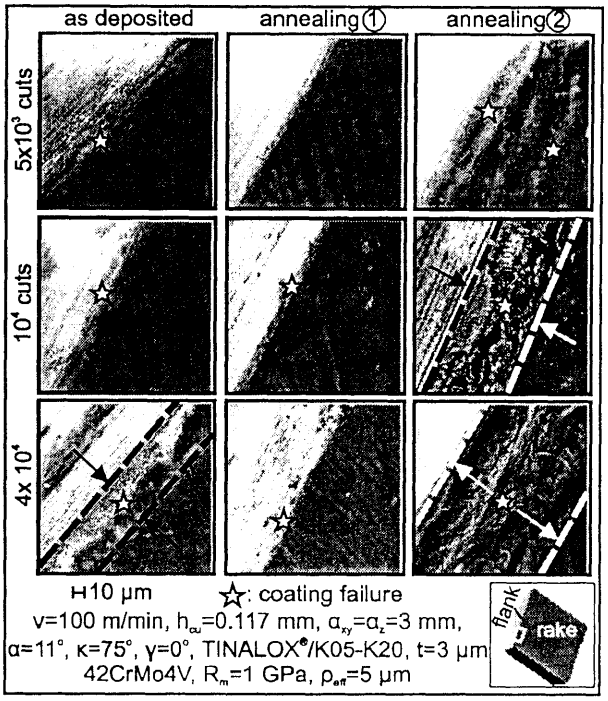

Figure 18: Coating fatigue failure and wear development at various annealing temperatures.

various wear stages are inserted. The first coating failure appears at the cutting wedge rounded area close to the flank /16/. The as deposited coating fails earlier than $5x10^3$ cuts, while in the case of annealing 1, a coating failure occurs later. The failure of the annealed 2 coating takes place earlier in comparison to the other two cases, the further wear development is more intense and the coating removal in the chip contact zone on the tool rake is remarkable.

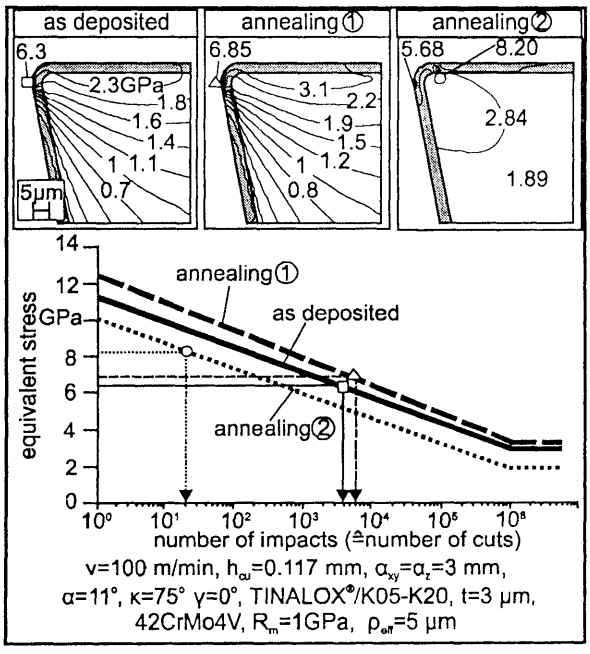

Figure 19: First coating failure and flank wear development of coated inserts annealed at various temperatures

The experimental results shown in figure 19 verify the previously mentioned tool wear behavior speculations. The annealed insert after annealing 2 cuts only approximately 10^3 times until a coating failure appears, whereas the as deposited coated tool managed to cut up to $4.5x10^3$ cuts. The annealed insert after annealing 1 managed to cut $7x10^3$ times up to the first coating failure. All these experimentally determined data are very close to the expected ones, according to the coating fatigue calculations, explained in the previous figure. The further wear development after the first coating failure, demonstrated in the lower diagram, exhibits again the superior wear behavior of the annealed coated insert after annealing 1, conducting almost 10^5 cuts up to a flank wear of 0.2 mm.

In order to analytically sustain the experimental results, FEM simulations of the contact between the cutting wedge and the workpiece material were conducted. At the upper part of figure 20 the von Mises equivalent stress distributions in the cutting wedge for the as deposited and the annealed 1,2 cases are demonstrated. The maximum developed equivalent stress in the as deposited and the annealed 1 cases appears at the cutting wedge rounded area close to the flank. On the other hand, the use of contact elements in the FEM simulation of the milling process /18/, to consider the adhesion problems in the case of annealed 2, revealed high occurred von Mises equivalent stresses on the tool rake face. Inserting the maximum developed stress values in the corresponding Woehler diagrams, the coating fatigue failure expectations during milling can be predicted. Hereby, the first coating failure for the as deposited insert is expected to occur approximately after $4x10^3$ successive cuts, whereas at annealing 1 and annealing 2 after $6x10^3$ and 20 cuts respectively. The

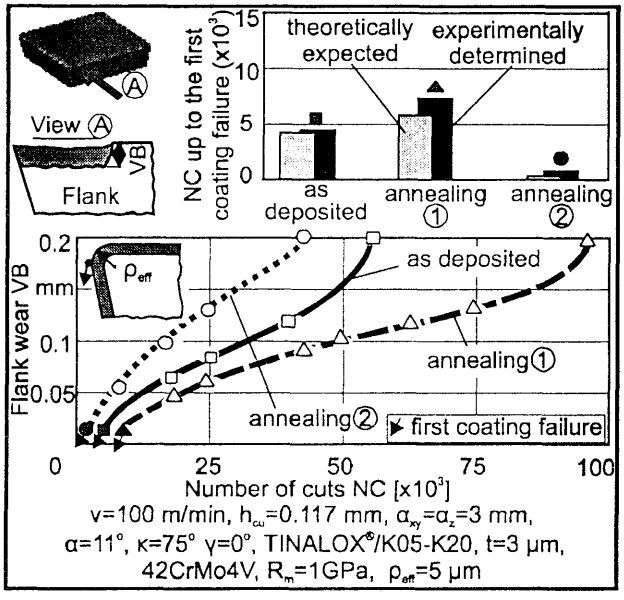

Figure 20: Stress distributions at the cutting wedge for various annealing temperatures and with their aid coating fatigue failure expectations during the milling process.

increased von Mises equivalent stresses on the tool rake face in the case of annealed 2, explains the early coating removal from the tool rake, demonstrated in figure 6.

9. Conclusions

In milling, ways to increase the cutting performance of coated tools were investigated. The first aim was to prevent the coating from premature failure. In this sense, a tool geometry optimization by increasing the cutting wedge effective radius leads to a superior performance of the cutting wedge as the conducted milling experiments clearly show. Moreover, the higher the developed stresses in the coating are the earlier the first coating failure appears and the more rapid the wear propagation develops. In the examined cases, the increasing of the undeformed chip thickness i.e. of the feedrate up to an optimum value appears to be beneficial for the tool service life. Furthermore coating annealing and substrate surface mechanical treatments may lead to higher cutting performance. These experimental results are also analytically sustained by FEM supported stress calculations and there is good agreement between the experimental and the computational ones. Finally the effect of the coating material on the tool performance was examined, with TINALOX® to have the superior performance both on HSS and HM substrates.

10. References

/1/ Klocke, F., "Coated Tools for Metal Cutting – Features and Applications", Key note paper, Annals of the CIRP, vol. 48, (1999), pp: 515-525.

/2/ Klocke, F., Krieg, T., Gerschwiler, K., Fritsch, R., Zinkann, V., Pohls, M., Eisenblaetter, G., "Improved cutting processes with adapted coating systems", Annals of the CIRP, vol. 47, (1998), pp: 65-68.

/3/ Bouzakis, K.-D., Vidakis, N., "Advanced physically vapour deposited coatings - state of the art innovations and future trends", Key note paper, Int. Journal Tribology in Industry, vol. 20, (1998), pp: 85-104.

/4/ Koenig, W., Fritsch, R., Kammermeier, G., "New approaches to characterizing the performance of coated cutting tools", Annals of the CIRP, vol. 41, (1992), pp: 49-54.

/5/ Toenshoff, H.-K., et. al., "PVD-coated tools for metal cutting applications", Proceedings of 1st int. conf. "THE Coatings" October 1999 Thessaloniki, (1999), pp: 1-20.

/6/ K.-D. Bouzakis, N. Michailidis, G. Erkens, Thin hard coatings stress-strain curves determination through a FEM supported evaluation of nanoindentation test results, in press in Surface and Coatings Technology, 2001.

/7/ HELMUT FISCHER GmbH +Co Evaluation Manual of Indentation Procedure, Germany Sindelfingen 2000.

/8/ K.-D. Bouzakis, N. Vidakis, K. David, 1999, The concept of an advanced impact tester supported by evaluation software for the fatigue strength characterization of hard layered media, Thin Solid Films, 355/356, (1999), 322-329.

/9/ K.-D. Bouzakis, N. Vidakis, T. Leyendecker, G. Erkens, R. Wenke, Determination of the fatigue properties of multilayer PVD coatings on various substrates, based on the impact test and its FEM simulation, Thin Solid Films, 308/309, (1997), 315-322.

/10/ Bouzakis, K.-D., Vidakis, N., Michailidis, N., Leyendecker, T., Erkens, G., Fuss, G., "Quantification of properties modification and cutting performance of (TixAl1-x)N coatings at elevated temperatures", Surface and Coating Technologies, vol. 120/121, (1999), pp: 34-43.

/11/ K.-D. Bouzakis, N. Michailidis, N. Vidakis, K. Efstathiou, T. Leyendecker, G. Erkens, R. Wenke, G. Fuss, Optimization of the cutting edge radius of PVD coated inserts in milling considering film fatigue failure mechanisms, Surface and Coatings Technology, 133/134, (2000), 501-507.

/12/ K.-D. Bouzakis, N. Michailidis, S. Hadjiyiannis, E. Pavlidou, G. Erkens, An effective way to improve the cutting performance of coated tools through annealing, in press in Surface and Coatings Technology, 2001.

/13/ SWANSON Analysis System, INC., ANSYS user manuals, Vol.1 Theory, Vol.2 Procedures, Vol.3 Elements, Vol.4 Commands, (1995).

/14/ Bouzakis, K. –D., Efstathiou, K., Vidakis, N., "The failure mechanism of PVD coated hardmetal inserts in milling", Int. Journal Tribology in Industry, vol. 19, (1997), pp: 93-102.

/15/ Brooks K., Word directory and handbook of hardmetals, 4th edition, international carbide data, (1987).

/16/ Bouzakis, K.-D., Vidakis, N., Kallinikidis, D., Leyendecker, T., Lemmer, O., Fuss, H.G., Erkens, G., "Fatigue failure mechanisms of multi- and mono- layer physically vapour deposited coatings in interrupted cutting processes", Surface and Coatings Technology, vol.108/109, (1998), pp: 526-534.

/17/ Bouzakis, K.-D., K. Efstathiou, N. Vidakis, D. Kallinikidis, S. Angos, T. Leyendecker, G. Erkens, H. Fuss, "Experimental and FEM analysis of the fatigue behaviour of PVD coatings on HSS substrate in milling", Annals of the CIRP, vol. 47, (1998), pp: 69-74.

/18/ K.-D. Bouzakis, N. Michailidis, K. Efstathiou, S. Hadjiyiannis, E. Pavlidou, G. Erkens, S. Rambadt, I. Wirth, "Improvement of PVD coated inserts cutting performance, through appropriate substrate and coating surface mechanical treatments", in press in Surface and Coatings Technology, 2001.

/19/ K.-D. Bouzakis, N. Michailidis, S. Hadjiyiannis, K. Efstathiou, E. Pavlidou, G. Erkens, S. Rambadt, I. Wirth, PVD coated inserts cutting performance improvement, by means of substrate and coating surface mechanical treatments, proceedings of the international conference "THE Coatings" in Manufacturing Engineering, held 9-10 May in Hannover, 2001, T5/1-10.

/20/ K.-D. Bouzakis, N. Michailidis, N. Vidakis, K. Efstathiou, S. Kompogiannis, G. Erkens, Interpretation of PVD coated inserts wear phenomena in turning, Annals of the CIRP, 49/1, (2000), 65-68.

/21/ K.-D. Bouzakis, N. Michailidis, N. Vidakis, K. Efstathiou, Failure mechanisms of physically vapour deposited coated hardmetal cutting inserts in turning, WEAR, 248, (2001), 29-37.

/22/ K.-D. Bouzakis, N. Michailidis, J. Anastopoulos, S. Kompogiannis, G. Erkens, P.J. Rudnik, PVD coated inserts cutting performance improvement, by means of substrate and coating surface mechanical treatments, proceedings of the international conference "THE Coatings" in Manufacturing Engineering, held 9-10 May in Hannover, 2001, T7/1-10.